Carbohydrate Polymers 89 (2012) 542–550

Contents lists available at SciVerse ScienceDirect

Carbohydrate Polymers

journal homepage: www.elsevier.com/locate/carbpol

Interaction study in homogeneous collagen/chondroitin sulfate blends by two-dimensional infrared spectroscopy

Huilin Tian[a], Yihui Chen[a,b], Cuicui Ding[a], Guoying Li[a,*]

[a] National Engineering Laboratory for Clean Technology of Leather Manufacture, Sichuan University, Chengdu 610065, PR China
[b] College of Chemistry and Chemical Engineering, Chongqing University of Science and Technology, Chongqing 401331, PR China

ARTICLE INFO

Article history:
Received 20 December 2011
Received in revised form 8 March 2012
Accepted 14 March 2012
Available online 23 March 2012

Keywords:
Collagen
Chondroitin sulfate
Hydrogen bond
Electrostatic interaction
Two-dimensional infrared correlation spectroscopy (2D IR)

ABSTRACT

The neutral homogeneous collagen/chondroitin sulfate (Col/CS) blends were prepared when using 0.25 mol/L NaCl to stabilize the blends. Composition-dependent Fourier transform-infrared (FTIR) spectra were analyzed by generalized two-dimensional (2D) correlation spectroscopy to investigate the conformational changes of collagen and the specific interactions between collagen and CS. When adding CS to the collagen solution, C–H bending vibration of collagen varies firstly, then collagen skeleton, and finally the specific interactions between collagen and CS. The Col/CS ratios influence the kinds of specific interactions. Only hydroxyl groups of CS interact with C=O group of collagen owing to the charge shielding effect of NaCl when the CS content is less than 50 wt%. Besides hydrogen bond, the electrostatic interactions between ionized carboxyl group or sulfate group of CS and ε-amino group of lysine or guanidine group of arginine appear when the CS content is more than 50 wt%.

1. Introduction

Chondroitin sulfate, which consists of a repeating disaccharide motif of glucuronic acid and N-acetyl-galactosamine, is a linear, complex, sulfated, polydisperse natural polysaccharide belonging to the class of macromolecules known as glycosaminoglycans (GAG) (Lamari and Karamanos, 2006; Maccari, Ferrarini, & Volpi, 2010). CS presents in all organisms from worms to humans (not in plants) and serves multiple important biological roles in particular as vital structural components of some connective tissues (Lauder, 2009). Consequently in order to protect the joint, CS is taken orally in capsules or tablets as a dietary supplement (Sakai, Otake, Toida, & Goda, 2007). What's more, CS is also used in eye drops, cosmetics and medical applications (Cohen, Wolfe, Mai, & Lewis, 2003; Kamata, Takahashi, Terajima, & Nishijima, 1995)., Collagen has shown superior advantages as biomaterials for tissue engineering as well as coating material for implants. However, the applications are more or less limited due to its relatively weak mechanical and thermal properties. In order to improve the corresponding performance, chemical crosslink or blending with other natural or synthetic macromolecule is adopted (Chen, Zhang, Liu, & Li, 2011; Freyman, Yannas, & Gibson, 2001; Kinneberg et al., 2010; Liang, Kienitz, Penick, Welter, Zawodzinski, & Baskaran, 2010; Pieper, Oosterhof, Dijkstra, Veerkamp, & van Kuppevelt, 1999; Zhang, Wu, & Li, 2011; Zhong et al., 2005). Among collagen-based copolymers, porous collagen/GAG scaffolds hold great potential for tissue engineering applications owing to a wealth of merits such as biological origin, non-immunogenicity, excellent biocompatibility and biodegradability (Keskin, Tezcaner, Korkusuz, Korkusuz, & Hasirci, 2005; Yannas, Burke, Gordon, Huang, & Rubenstein, 1980). In addition, the attachment of GAG to collagen facilitates the study of biocharacteristics of these polysaccharides (Pieper et al., 1999; Zhong et al., 2005). It is noteworthy that combining CS with collagen is unique in skin regeneration to reduce scar formation (Freyman et al., 2001). Moreover, after incorporating CS into a collagen scaffold, the resultant biomaterial has been endowed advantages such as the enhancement of cell attachment, migration, division and stiffness of the resultant matrix (Hua, Li, Zhou, & Gao, 2011; van Susante et al., 2001; Wollenweber et al., 2006).

Despite the biological advantages of Col/CS scaffolds, the homogeneity of the blends and the influence of the Col/CS weight ratio on the interactions between them are usually ignored. In general, the Col/CS scaffolds are produced by lyophilizing Col/CS-acetic acid solutions and the Col/CS weight ratio is usually 91/9 (Keskin et al., 2005; Kinneberg et al., 2010; Liang et al., 2010). However, there is no relevant literature to prove whether this ratio is optimum till now. Moreover, when blending CS with collagen in acetic acid solution, the Col/CS co-precipitation appears immediately because of the strong electrostatic interaction between positively charged collagen and anionic CS, resulting in the heterogeneous Col/CS

* Corresponding author. Tel.: +86 028 85462568; fax: +86 028 85405237.
E-mail address: liguoyings@163.com (G. Li).

0144-8617/$ – see front matter © 2012 Elsevier Ltd. All rights reserved.
doi:10.1016/j.carbpol.2012.03.042

blends. According to the researches that the increase of collagen concentration improves the mechanical properties of scaffold obviously (Liang et al., 2010) and accelerates the collagen self-assembly (Yan et al., 2012), it is inferred that the physicochemical properties of a solution might correlate with the mechanical and biological properties of the resultant biomaterial. What's more, even for a settled scaffold, its physical, chemical and biological properties must be optimized for the targeted tissue. Therefore, the mechanical or biological properties of Col/CS scaffolds might be optimized through preparing homogenous Col/CS blends and changing the Col/CS ratios. Then the focus is firstly placed on how to prepare homogenous Col/CS blends with various Col/CS ratios. As a result of charge shielding effect of NaCl, sodium chloride aqueous solution is finally adopted to stabilize the Col/CS blends for this experiment. In addition the concentration of NaCl will be judged according to the miscibility of blends revealed by the viscosity measurement.

The nature of interactions occurring between collagen and CS bears great physiologic and pathologic importance. However, the chemical binding of CS to collagen is still not fully understood and yet to be explored. It has been accepted that the interaction between collagen and CS is usually of electrostatic nature under physiological ionic strength and pH value (Gelman and Blackwell, 1973; Öbrink and Wasteson, 1971) and strongly dependent on the ionic strength of the medium (Öbrink, Laurent, & Carlsson, 1975). Therefore the electrostatic interaction between them is abolished when the ionic strength is up to 0.4 (Öbrink, 1973). However, as pointed out by Munakata, the interaction between collagen and GAG was not influenced by the presence of Ca^{2+} and Mg^{2+} (Munakata, Takagaki, Majima, & Endo, 1999). Thus it suggests that the interactions between collagen and CS involve not only electrostatic binding, but also other types of specific interaction such as hydrogen bond.

2D correlation spectroscopy, which is successful in systematically extracting the specific nature of spectral intensity variations induced by an external perturbation (Noda, 1990, 1993, 2006), has been applied as an effective tool to study interactions at molecular level in various kinds of systems such as polymer blends (Huang, Malkov, Coleman, & Painter, 2003). According to Ren's work, the conformational changes and specific interactions in the blends of atactic polystyrene (PS) and poly (2,6-dimethyl-1,4-phenylene ether) (PPE) have been analyzed by generalized 2D FT-Raman correlation spectroscopy (Ren, Murakami, Nishioka, Nakashima, Noda, & Ozaki, 1999). By spreading spectral peaks over the second dimension, the visualization of complex spectra consisting of many overlapped bands is identified and the spectra resolution is enhanced. Thus according to Noda's rules (Noda, 1990, 1993, 2006; Ren et al., 1999), the bands of CS can be differentiated from those of collagen in the highly overlapped spectra of the blends by synchronous correlation analysis of the FTIR spectra. Synchronous cross-peak $\Phi[\nu_1,\nu_2]$ indicates simultaneous or coincidental changes of the two bands at ν_1 and ν_2 as the function of external perturbation. The sign of $\Phi[\nu_1,\nu_2]$ becomes positive if the intensities of bands at ν_1 and ν_2 are either increasing or decreasing together when subjected to the external perturbation. As to the negative sign of $\Phi[\nu_1,\nu_2]$, it means one band is increasing while the other is decreasing when subjected to the external perturbation. It is obvious that the band intensities of collagen decrease while those of CS increase as Col/CS ratios changing from 100/0 to 9/91. Therefore the bands could be ascribed unambiguously to collagen or CS according to the rules as follows: $\Phi[\nu_1(\text{collagen}),\nu_2(\text{collagen})] > 0$, $\Phi[\nu_1(\text{collagen}),\nu_2(\text{CS})] < 0$, $\Phi[\nu_1(\text{CS}),\nu_2(\text{collagen})] < 0$ and $\Phi[\nu_1(\text{CS}),\nu_2(\text{CS})] > 0$.

An asynchronous cross-peak $\Psi[\nu_1,\nu_2]$ appears only when the intensities of two bands at ν_1 and ν_2 vary dissimilarly or out of phase. With respect to the present work, the direct proportional changes of band intensities caused by the composition variations in the Col/CS blends alone should not give rise to an asynchronous cross-peak. Therefore the appearance of $\Psi[\nu_1,\nu_2]$ means the bands at ν_1 and ν_2 are subjected to additional influences induced by local structural changes or molecular interactions. For example, the intensity of C=O stretching vibration due to collagen and the intensity of O–H stretching vibration assigned to CS are influenced not only by Col/CS ratios but also by the interaction between them and then an asynchronous cross-peak between the corresponding two bands might develop.

The asynchronous spectrum also offers complementary information to the synchronous spectrum and the sign of $\Psi[\nu_1,\nu_2]$ gives information about the sequential order of changes at ν_1 and ν_2. According to Noda, if the signs of $\Phi[\nu_1,\nu_2]$ and $\Psi[\nu_1,\nu_2]$ are the same, ν_1 varies prior to ν_2 and it implies that ν_1 changes at lower CS content compared to ν_2 in the present work. If the signs of $\Phi[\nu_1,\nu_2]$ and $\Psi[\nu_1,\nu_2]$ are opposite, ν_1 varies after ν_2 and it suggests that ν_1 changes at higher CS content than ν_2 (Noda, 1989, 2006).

In the present work, FTIR and generalized 2D IR correlation analysis were applied to study the conformational changes of collagen and the molecular interactions between collagen and CS in homogeneous blends. In addition, the composition-dependent FTIR spectra were analyzed by 2D correlation analysis to investigate the kinds of interactions in the presence of different amount of CS.

2. Experimental

Collagen was extracted in our laboratory from calf skins by pepsin digestion according to the previously described method (Zhang, Li, & Shi, 2006). After dialyzing against 0.1 mol/L acetic acid for three days, the acidic collagen solution was lyophilized by a freeze dryer (Labconco Freeze Dryer FreeZone 6 Liter, USA) at −40 °C for two days. Chondroitin sulfate (from bovine cartilage) was purchased from Yibao Biotech Ltd. (Shandong, China) and had average molecular weights of 20KDa. Both the freeze-dried collagen and chondroitin sulfate were stored at 4 °C until required.

2.1. Preparations of blends

The NaCl aqueous solution at pH 7.4 with a concentration of 0.25 mol/L was initially prepared in the present work. Then CS was dissolved in it to obtain a solution with a concentration of 5 mg/mL. During the dissolving process of collagen in 0.25 mol/L NaCl, 0.5 mol/L NaOH was dripped into the solution to adjust the pH value remaining ~7.4 and the final concentration was 5 mg/mL. Before blending with CS, the collagen solution was degassed by centrifugation at 15,000 × *g* for 10 min and dialyzed against 0.25 mol/L NaCl for three days. The Col/CS blends were produced by mixing suitable volumes of collagen and CS aqueous solution and stored overnight at 4 °C after stirring for 6 h. The final weight ratios of Col/CS blends with pH 7.21–7.28 were as follows: 100/0, 91/9, 80/20, 70/30, 50/50, 30/70, 20/80 and 9/91. All manipulations were carried out on ice.

2.2. Viscometry of the Col/CS blends

Viscosity measurements of collagen, CS and Col/CS blend solutions were conducted in 0.25 mol/L NaCl at (25.0 ± 0.01) °C, using a wsn-1 Ubbelohde-type capillary viscometer. The initial solutions for the measurements were prepared by diluting the stock solutions described in Section 2.1 with 0.25 mol/L NaCl and the concentration was 0.2 mg/mL when the CS content is less than 50 wt% and 0.5 mg/mL when the CS content is more than 50 wt%, respectively. Various dilutions to yield four lower concentrations required during the viscosity measurements were carried out in the bulb of the viscometer. Measurements started after an equilibration time of 20 min. The efflux time of each solution was the average of five

measurements and the difference of each result was confined to less than 0.2 s. For calculation of miscibility, the procedures are listed in the literature (García, Melad, Gómez, Figueruelo, & Campos, 1999; Jiang and Han, 1998) and the mainly used equations are shown as follows:

$$\frac{[\eta]_{sp,m}}{C_{Col}+C_{CS}} = [\eta]_m^{exp} + b_m(C_{Col}+C_{CS}) \quad (1)$$

where $[\eta]_{sp,m}$ is the specific viscosity of the blends, C_{Col} and C_{CS} are the concentrations of collagen and CS in the blends respectively, $[\eta]_m^{exp}$ is the intrinsic viscosity of the blends determined experimentally and b_m is the viscometric interaction parameter.

$$[\eta]_m^i = [\eta]_{Col}\omega_{Col} + [\eta]_{CS}\omega_{CS} \quad (2)$$

where $[\eta]_m^i$ is the ideal intrinsic viscosity of the blends, $[\eta]_{Col}$ and $[\eta]_{CS}$ are the intrinsic viscosities of collagen and CS respectively, and ω_{Col} andω_{CS} are the weight fraction of collagen and CS in the blends respectively.

The criterion for compatibility in the blends is based on the comparison between $[\eta]_m^{exp}$ and $[\eta]_m^i$. If $[\eta]_m^{exp}$ represents a smaller value than $[\eta]_m^i$, the blends are compatible, considering the existence of attractive interaction. On the other hand, if $[\eta]_m^{exp}$ shows a larger value than $[\eta]_m^i$, the blends are incompatible.

2.3. FTIR measurements

The samples for FTIR measurements were produced by lyophilizing the stock solutions mentioned in Section 2.1 at −40 °C for two days and stored in a silica gel desiccator for five days before testing to reduce the influence of water. The samples were triturated with potassium bromide (KBr) in the ratio of 1:100 (mg/mg) and prepared as pellets. The FTIR spectra were recorded at a resolution of 4 cm^{-1} at room temperature using a Nicolet iS10 spectrometer (Thermo Fisher Scientific, USA) and 32 scans were performed for each spectrum.

2.4. 2D FTIR correlation analysis

The series of perturbation-dependent spectra were obtained by varying compositions of the blends of collagen and CS. To investigate the interactions in detail by 2D correlation analysis, the FTIR spectra had been divided into two sets: set A of low CS content and set B of high CS content. Set A contained five spectra: those of Col/CS = 100/0, 91/9, 80/20 and 70/30 wt%. Set B contained five spectra: those of Col/CS = 50/50, 30/70, 20/80 and 9/91 wt%.

Before 2D correlation analysis, the spectra were subjected to slightly 5-point smoothing and baseline correction by Omnic 8. The calculation of the generalized 2D correlation spectra was based on the software 2D Pocha (developed by Daisuke Adachi, Kwansei-Gakuin University, Japan). Visualization of the 2D IR correlation contour maps was performed with the use of Origin 7.5 software, where the regions with solid and dashed lines indicated positive and negative correlation intensities, respectively.

3. Results and discussion

3.1. Miscibility of the Col/CS blends

Miscibility of the components in polymer blends is an important aspect of the properties and assigned to specific interactions between polymeric components. One kind of the most common interactions in the blends is hydrogen bond (Sionkowska, Wisniewski, Skopinska, Kennedy, & Wess, 2004). The viscometric data for binary blends containing collagen and CS are shown in Table 1.

Table 1
Viscometric data for binary blends containing collagen and CS.

Blend ratio (wt%) Col/CS	$[\eta]_m^i$ (mL/g)	$[\eta]_m^{exp}$ (mL/g)	Miscibility
91/9	698.37	514.01	Miscible
80/20	617.21	467.44	Miscible
50/50	394.04	307.63	Miscible
20/80	170.86	80.02	Miscible
9/91	89.70	36.91	Miscible

According to the results in Table 1, $[\eta]_m^{exp}$ exhibits smaller value than $[\eta]_m^i$, suggesting the miscibility of the blends and the occurrence of attractive interaction. It means that the concentration of NaCl is enough to prepare homogeneous blends as a result of the charge shielding effect of NaCl. The specific interactions between collagen and CS in neutral blends with different amount of CS will be discussed in the following sections.

3.2. IR spectra of Col/CS blends

Fig. 1 shows the IR spectra of pure collagen, pure CS and Col/CS blended samples. As shown in Table 2, the assignments of absorption peaks associated with major functional groups of collagen are based upon Sionkowska's, Wisniewski's and Chen's works (Chen, Mo, He, & Wang, 2008; Sionkowska et al., 2004; Wisniewski, Sionkowska, Kaczmarek, Lazare, Tokarev, & Belin, 2007); the assignments of absorption bands of CS are based on the Sadtler standard IR spectra handbook (Bio-Rad Laboratories, Inc. U.S.) and the reports written by Maruyama, Toida, Imanari, Yu, & Linhardt (1998) and Zheng, Guan, & Huang (2008).

The IR spectrum of type I collagen is dominated by the contributions arising from vibrations of the amide groups and the characteristic bands at 1660, 1548 and 1239 cm^{-1} represent the amide I, II and III bands of collagen, respectively. The amide I band of collagen arises predominantly from amide C=O stretching vibrations and the amide II band arises from amide N–H bending vibration and C–N stretching vibration. Compared with the amide I and II absorption, the source of amide III peak at 1239 cm^{-1} seems to be more complex, consisting of components from C–N stretching and N–H in plane bending from amide linkages, as well as absorptions assigned to wagging vibrations of CH_2 groups from the glycine backbone and proline side-chains (Sionkowska et al., 2004).

As to CS, the bands at 1377 and 1416 cm^{-1} represent C=O and C–O stretching vibration of ionized carboxyl group, respectively, and the bands at 1066 and 1127 cm^{-1} represent C–O stretching vibration of hydroxyl groups. It is noteworthy that the

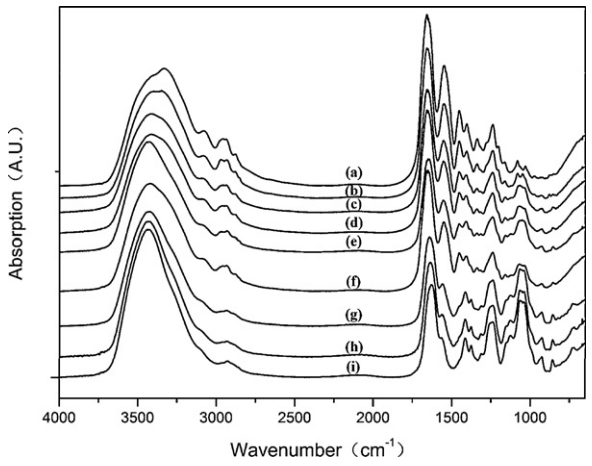

Fig. 1. FTIR spectra for (a) collagen, (i) CS and Col/CS blends at ratios of (b) 91/9, (c) 80/20, (d) 70/30, (e) 50/50, (f) 30/70, (g) 20/80 and (h) 9/91.

Table 2
Assignments of the bands in the FTIR spectra of collagen and CS.

Collagen		CS	
Frequency (cm^{-1})	Assignment	Frequency (cm^{-1})	Assignment
3350	N–H stretching vibration, coupled with hydrogen bonding	3424	N–H stretching + O–H stretching vibrations
3080	C–H stretching vibration	2926	C–H stretching vibration
2958	$-CH_2$ asymmetric stretching	1628	C=O stretching vibration
1660	C=O stretching + C–N stretching + N–H bending vibrations	1560	N–H bending vibration
1548	N–H bending + C–N stretching vibrations	1416	C–O stretching vibrations
1453	CH_3 asymmetric bending vibration	1377	C=O symmetric bending vibration
1404	C–H deformation	1310	C–O bending vibrations
1338	CH_3 wagging of proline	1239	S=O stretching vibration
1239	C–N stretching + in-plane N–H bending + CH_3–C stretching vibrations	1127	C–O stretching vibrations
1164	CH_2 wagging	1066	C–O stretching vibrations
1082	Skeletal C–C–C asymmetric stretching vibration	928	Pyranose ring asymmetric stretching vibration
1030	In-plane C–H deformation	856	$-O-SO_3$ stretching + –C–O–S stretching vibrations
972	C–O stretching	726	$-O-SO_3$ stretching + –C–O–S stretching vibrations

characteristic absorption peaks of CS include not only C=O and O–H stretching vibration, but also S=O stretching vibration located at about 1239 cm^{-1} (Garnjanagoonchorn, Wongekalak, & Engkagul, 2007).

According to the IR spectra of collagen and CS, some positions of their absorption bands are very close to each other and as a result it is difficult to ascribe bands in the spectra of the blends to collagen or CS. Nevertheless small changes are revealed in the spectra as a result of the variation of Col/CS ratios. The amide I band of collagen shifts from 1660, 1651 to 1640 cm^{-1} and the intensity of amide II band decreases as well with Col/CS ratios changing from 100/0, 50/50 to 20/80. As the amide I band of collagen is sensitive to the change of secondary structure, the distinct shifts of the band positions in the Col/CS blends suggest the conformational change of collagen and the existence of interactions between collagen and CS. However, the IR spectra can provide no further information and then 2D correlation analysis is required. Meanwhile more attention was paid to the spectrum range between 1750 cm^{-1} and 980 cm^{-1} in the following discussion in view of the main absorption bands of both collagen and CS. In addition in order to facilitate the 2D correlation analysis, the range between 1750 cm^{-1} and 980 cm^{-1} was divided into three parts: 1750–1480 cm^{-1}, 1480–1280 cm^{-1} and 1280–980 cm^{-1}.

3.3. 2D correlation FTIR spectra of Col/CS blends

The 2D synchronous and asynchronous FTIR correlation spectra of set A and set B in the range of 1750–1480 cm^{-1} and 1280–980 cm^{-1} are depicted in Fig. 2. In the synchronous plots (Fig. 2A and C), the auto-peak located at 1528 cm^{-1} is due to the intensity reduction of amide II band of collagen, as seen in Fig. 1. Therefore according to the rules described above, the positive cross-peaks at (1690, 1528) and (1614, 1528) in Fig. 2A indicates that the bands at 1690 and 1614 cm^{-1} are due to collagen in set A. In Fig. 2C the positive cross-peak at (1690, 1528) implies that the band at 1690 cm^{-1} is also ascribed to collagen, however, the negative cross-peak at (1614, 1528) suggests that the band at 1614 cm^{-1} is assigned to CS in set B. Comparing Fig. 2B with Fig. 2D, it is noteworthy that there are strong negative asynchronous cross-peaks at (1690, 1528) and (1614, 1528) in Fig. 2B, while in Fig. 2D the cross-peak at (1690, 1528) disappears and the positive cross-peak at (1614, 1528) also remains. It supposes that the C=O group of CS might replace that of collagen to form molecular hydrogen bond with amino group of collagen when the content of CS is more than 50 wt%.

The synchronous 2D FTIR spectrum in the 1280–850 cm^{-1} range (Fig. 2E and G) shows a strong auto-peak at 1050 cm^{-1} which obviously arises from CS. Furthermore, this assignment is confirmed by the negative correlation peaks at (1690, 1050) and (1528, 1050) in the synchronous plots between 1750–1480 cm^{-1} and 1280–850 cm^{-1} ranges (shown in Fig. 3A and C). Then the negative synchronous cross-peaks at (1239, 1050) and (1200, 1050) in Fig. 2E indicate that the bands at 1239 and 1200 cm^{-1} are assigned to amide III band of collagen in set A, however, the positive cross-peaks at (1239, 1050) and (1260, 1050) in Fig. 2G indicate that the bands at 1239 and 1260 cm^{-1} are due to the S=O stretching vibration in the sulfate group of CS in set B. The negative synchronous cross-peaks at (1239, 1127) and (1200, 1127) in Fig. 2E and the positive synchronous cross-peaks at (1239, 1127) and (1200, 1127) in Fig. 2G suggest that the band at 1127 cm^{-1} is also derived from CS. Therefore it can draw a preliminary conclusion that the sulfate group of CS does not interact with cationic residues of collagen via electrostatic interaction in set A and the specific kind of interaction will be discussed later. As to set B, although the bands at 1239 and 1200 cm^{-1} have been ascribed to CS, the specific electrostatic interaction between collagen and CS can not be ascertained accordingly.

Fig. 3A and B presents the 2D correlation spectrum of set A between the ranges 1750–1480 cm^{-1} and 1280–980 cm^{-1}. The six negative synchronous and asynchronous cross-peaks at (1690, 1127), (1690, 1050), (1614, 1127), (1614, 1050), (1528, 1127) and (1528, 1050) are thought to reflect the specific interaction between collagen and CS in set A. In addition, the positive synchronous cross-peaks at (1690, 1200), (1690, 1239), (1528, 1200) and (1528, 1239) confirm the bands at 1200 and 1239 cm^{-1} are due to collagen again. Therefore it means that in set A only the hydroxyl groups of CS interact with the C=O groups of collagen via hydrogen bonding because the bands at 1050 and 1127 cm^{-1} represent C–O stretching vibration of the C–OH groups and the sulfate group of CS is not involved in the interaction between collagen and CS in set A.

Fig. 3C and D shows the 2D correlation spectrum of set B between the ranges 1750–1480 cm^{-1} and 1280–980 cm^{-1}. It is noteworthy that besides the four asynchronous negative cross-peaks at (1690, 1127), (1690, 1050), (1528, 1127) and (1528, 1050) also shown in Fig. 3A and B, there appear another four asynchronous negative cross-peaks at (1690, 1239), (1690, 1260), (1528, 1239) and (1528, 1260), respectively. The negative synchronous cross-peaks at (1690, 1260), (1690, 1239), (1528, 1260) and (1528, 1239) indicate the bands at 1260 and 1239 cm^{-1} are ascribed to the S=O stretching vibration of sulfate group of CS in set B. Here, the asynchronous cross-peaks are thought to reflect the specific electrostatic interactions between cationic residues of collagen and sulfate group of CS.

According to Table 2, the C–O stretching vibration and C=O symmetric stretching vibration of ionized carboxyl group of CS locate at 1416 cm^{-1} and 1377 cm^{-1}, respectively, and the vibration

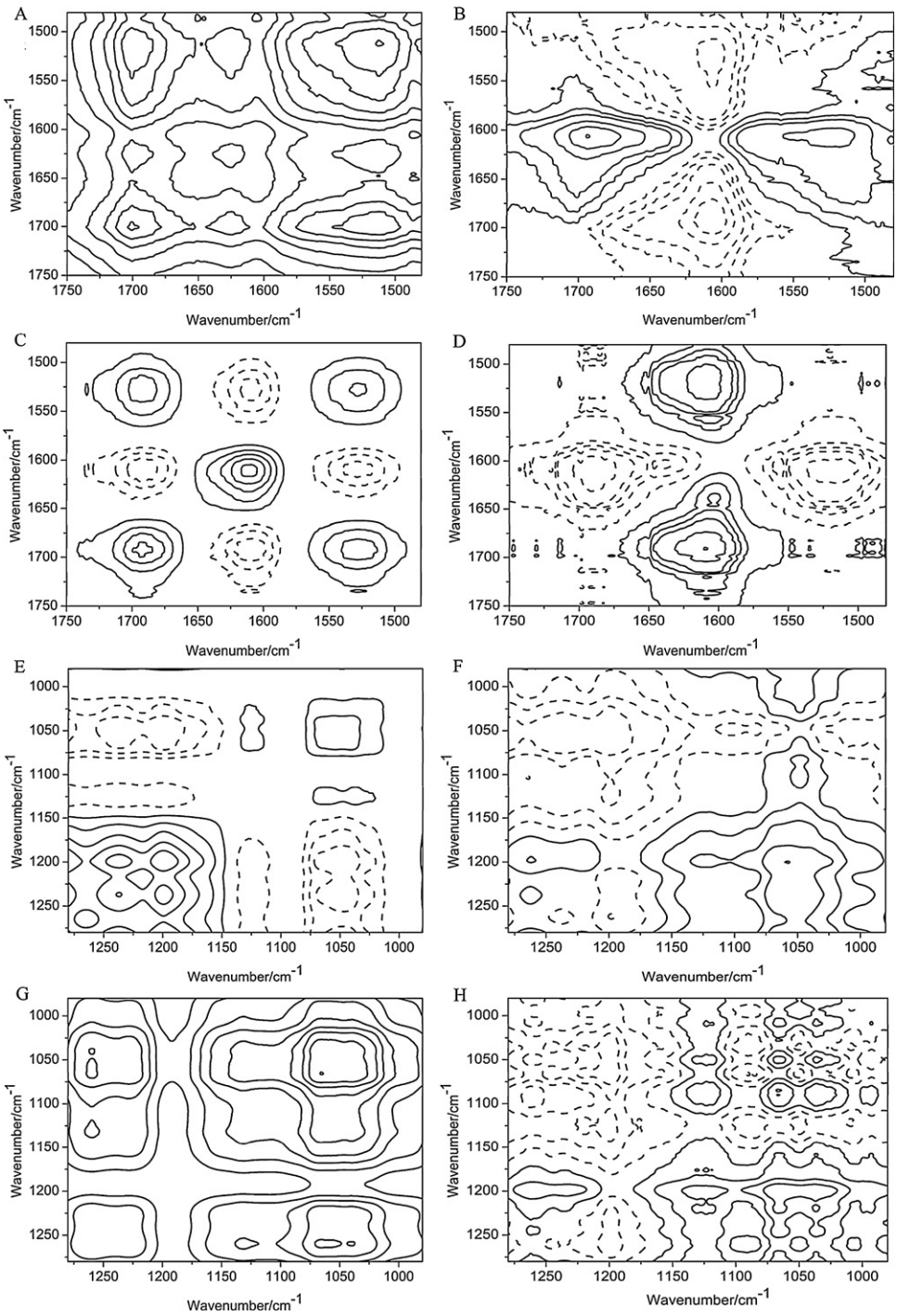

Fig. 2. Synchronous (A, C, E, G) and asynchronous (B, D, F, H) 2D correlation spectra in the region: (A–D) 1750–1480 cm^{-1}, and (E–H) 1280–980 cm^{-1}. A, B, E, F were constructed from the spectra of set A and C, D, G, H were constructed from set B.

intensity of C–O and C=O stretching must be influenced by electrostatic interaction between ionized carboxyl group of CS and cationic residues of collagen. Thus the 2D correlation analysis between the range 1750–1480 cm^{-1} and 1480–1280 cm^{-1} (shown in Fig. 4) can be used to judge if this kind of electrostatic interaction occurs or not. The variation order between two bands of set A is listed in Table 3 and that of set B is listed in Table 4.

As shown in Fig. 4A, all the positive synchronous cross-peaks indicate that the bands at 1454, 1400 and 1336 cm^{-1} are due to collagen and the bands ascribed to the vibration of ionized carboxyl group of CS do not develop cross-peaks with cationic groups of collagen in Fig. 4B. It means the electrostatic interaction between ionized carboxyl group of CS and cationic residues of collagen is also absent in set A.

Based on the results shown in Figs. 2–4 and Table 3, the variation order of bands in set A is as follows: 1454 cm^{-1} > 1239 cm^{-1} > 1528 cm^{-1} > 1614 cm^{-1} > 1690 cm^{-1} > 1050 cm^{-1} > 1127 cm^{-1}, in which the later one prefers to occur at higher CS content than the former one. In other words, C–H bending vibration of collagen at 1454 cm^{-1} changes firstly at lowest CS content when blending CS with collagen. The variation of collagen backbone takes place subsequently because

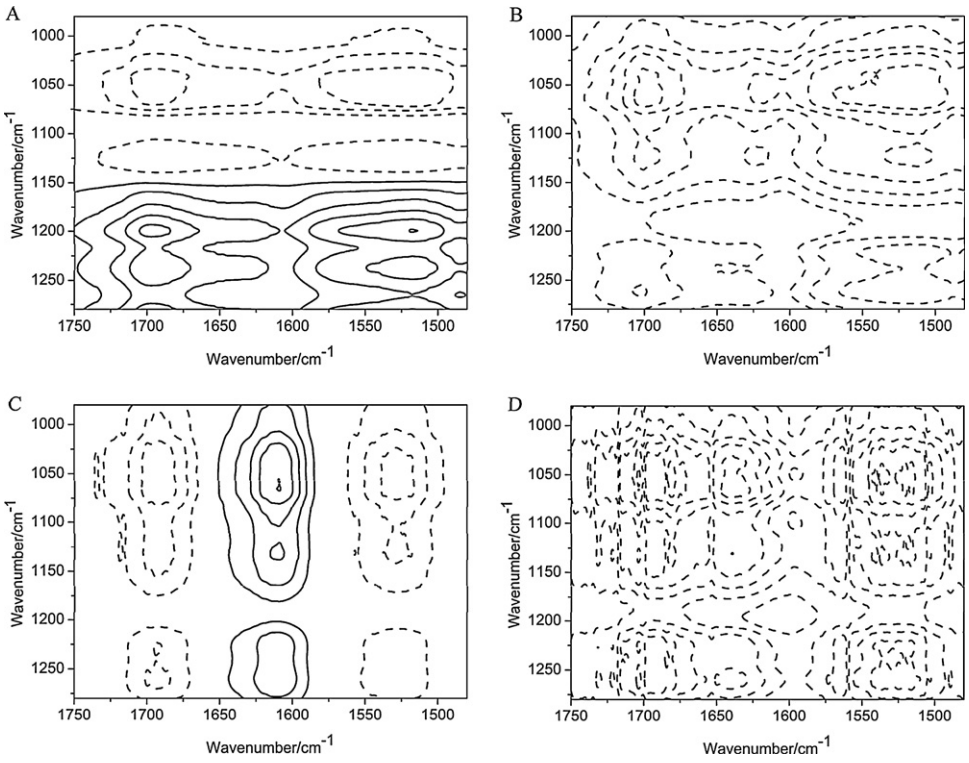

Fig. 3. Synchronous (A and C) and asynchronous (B and D) 2D correlation spectra in the range 1750–1480 cm^{-1} vs. 1280–980 cm^{-1}, A and B constructed from the spectra of set A and C and D constructed from set B.

the amide I, II and III bands of collagen are directly related to the conformation of polypeptide backbone (Thomas, Dean, & Jose, 2007). Finally the hydrogen bond between C=O group of collagen and hydroxyl group of CS occurs.

As shown in Fig. 4C, the negative synchronous cross-peaks at (1690, 1416), (1690, 1377), (1528, 1416) and (1528, 1377) suggest the bands at 1416 and 1377 cm^{-1} are assigned to CS and the corresponding negative asynchronous cross-peaks imply the

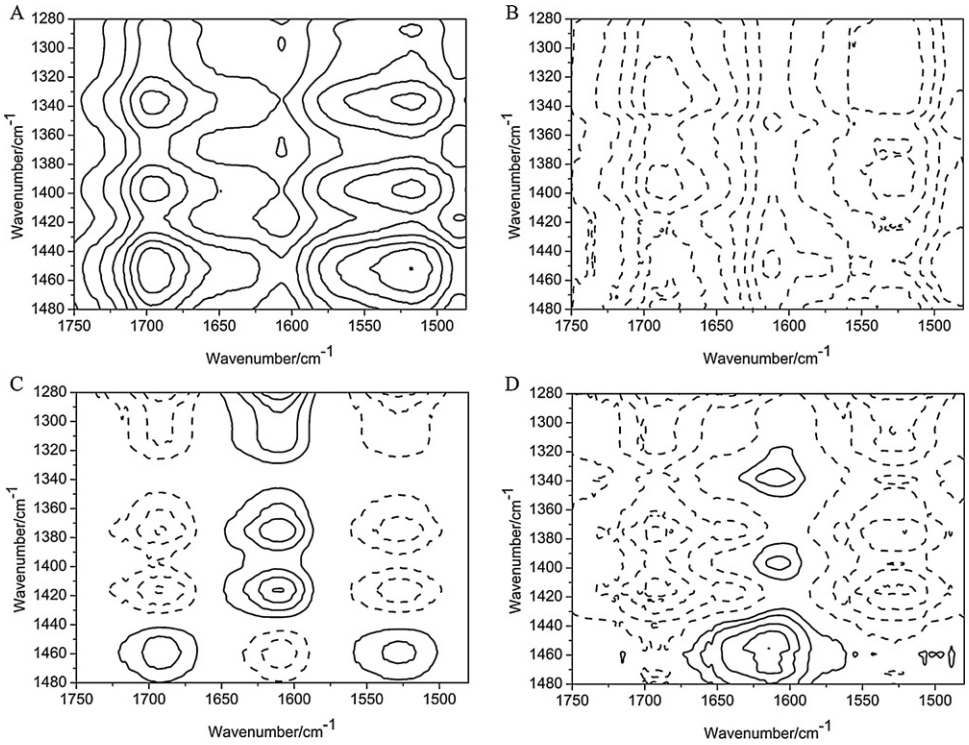

Fig. 4. Synchronous (A and C) and asynchronous (B and D) 2D correlation spectra in the range 1750–1480 cm^{-1} vs. 1480–1280 cm^{-1}, A and B constructed from the spectra of set A and C and D constructed from set B.

Table 3
Synchronous, asynchronous 2D correlation intensities and the order of intensity variations between two bands in Set A.

No.	Φ	Ψ	Assignment	Order[a]
1	$\Phi(1690,1614)>0$	$\Psi(1690,1614)<0$	(COL, COL)	1690 after 1614 cm^{-1}
2	$\Phi(1690,1528)>0$	$\Psi(1690,1528)<0$	(COL, COL)	1690 after 1528 cm^{-1}
3	$\Phi(1614,1528)>0$	$\Psi(1614,1528)<0$	(COL, COL)	1614 after 1528 cm^{-1}
4	$\Phi(1239,1050)<0$	$\Psi(1239,1050)<0$	(COL, CS)	1239 before 1050 cm^{-1}
5	$\Phi(1200,1050)<0$	$\Psi(1206,1050)<0$	(COL, CS)	1200 before 1050 cm^{-1}
6	$\Phi(1239,1127)<0$	$\Psi(1239,1127)<0$	(COL, CS)	1239 before 1127 cm^{-1}
7	$\Phi(1200,1127)<0$	$\Psi(1206,1127)<0$	(COL, CS)	1200 before 1127 cm^{-1}
8	$\Phi(1690,1127)<0$	$\Psi(1690,1127)<0$	(COL, CS)	1690 before 1127 cm^{-1}
9	$\Phi(1690,1050)<0$	$\Psi(1690,1050)<0$	(COL, CS)	1690 before 1050 cm^{-1}
10	$\Phi(1528,1127)<0$	$\Psi(1528,1127)<0$	(COL, CS)	1528 before 1127 cm^{-1}
11	$\Phi(1528,1050)<0$	$\Psi(1528,1050)<0$	(COL, CS)	1528 before 1050 cm^{-1}
12	$\Phi(1690,1239)>0$	$\Psi(1690,1239)<0$	(COL, COL)	1690 after 1239 cm^{-1}
13	$\Phi(1614,1239)>0$	$\Psi(1614,1239)<0$	(COL, COL)	1614 after 1239 cm^{-1}
14	$\Phi(1528,1239)>0$	$\Psi(1528,1239)<0$	(COL, COL)	1528 after 1239 cm^{-1}
15	$\Phi(1690,1454)>0$	$\Psi(1690,1454)<0$	(COL, COL)	1690 after 1454 cm^{-1}
16	$\Phi(1690,1400)>0$	$\Psi(1690,1400)<0$	(COL, COL)	1690 after 1400 cm^{-1}
17	$\Phi(1528,1454)>0$	$\Psi(1528,1454)<0$	(COL, COL)	1528 after 1454 cm^{-1}
18	$\Phi(1528,1400)>0$	$\Psi(1528,1400)<0$	(COL, COL)	1528 after 1400 cm^{-1}
19	$\Phi(1454,1200)>0$	$\Psi(1454,1200)<0$	(COL, COL)	1454 after 1200 cm^{-1}
20	$\Phi(1454,1239)>0$	$\Psi(1454,1239)<0$	(COL, COL)	1454 after 1239 cm^{-1}
21	$\Phi(1454,1127)<0$	$\Psi(1454,1127)<0$	(COL, CS)	1454 before1127 cm^{-1}
22	$\Phi(1454,1050)<0$	$\Psi(1454,1050)<0$	(COL, CS)	1454 before1050 cm^{-1}

[a] ν_1 after (before) ν_2 means the intensity change of the band at ν_1 occurs at higher (lower) CS contents than that at ν_2.

ionized carboxyl group of CS interacts with cationic residues of collagen through electrostatic interaction in set B. According to Table 4, the variation order of bands of CS in set B is listed as follows: 1050 cm^{-1} > 1127 cm^{-1} > 1239 cm^{-1} > 1416 cm^{-1}. In other words, CS interacts with collagen through hydrogen bond between hydroxyl group of CS and C=O group of collagen firstly, then the electrostatic interaction between sulfate group of CS and cationic residues of collagen, and finally the electrostatic interaction between carboxyl group of CS and cationic residues of collagen.

Both the sulfate and carboxyl groups of CS might interact via electrostatic interactions with cationic residues of collagen because they are ionized at neutral pH (Gelman and Blackwell, 1973). However, the electrostatic interaction between polyelectrolyte of opposite charge depends on the strength of the alkaline or the acidic sites they bear and their charge density (Denuziere, Ferrier, & Domard, 1996). In addition the net charge of collagen is small because this selected pH value is close to the isoelectric point of collagen and in the presence of NaCl at the concentration of 0.25 M

Table 4
Synchronous, asynchronous 2D correlation intensities and the order of intensity variations between two bands in Set B.

No.	Φ	Ψ	Assignment	Order[a]
1	$\Phi(1690,1614)<0$	$\Psi(1690,1614)<0$	(COL, CS)	1690 before 1614 cm^{-1}
2	$\Phi(1614,1528)<0$	$\Psi(1614,1528)>0$	(COL, CS)	1614 after 1528 cm^{-1}
3	$\Phi(1260,1050)>0$	$\Psi(1260,1050)<0$	(CS, CS)	1260 after 1050 cm^{-1}
4	$\Phi(1260,1127)>0$	$\Psi(1260,1127)<0$	(CS, CS)	1239 after 1127 cm^{-1}
5	$\Phi(1690,1239)<0$	$\Psi(1690,1239)<0$	(COL, CS)	1690 before 1239 cm^{-1}
6	$\Phi(1690,1260)<0$	$\Psi(1690,1260)<0$	(COL, CS)	1690 before 1260 cm^{-1}
7	$\Phi(1690,1127)<0$	$\Psi(1690,1127)<0$	(COL, CS)	1690 before 1127 cm^{-1}
8	$\Phi(1690,1050)<0$	$\Psi(1690,1050)<0$	(COL, CS)	1690 before 1050 cm^{-1}
9	$\Phi(1614,1239)>0$	$\Psi(1690,1239)<0$	(CS, CS)	1614 after 1239 cm^{-1}
10	$\Phi(1614,1260)>0$	$\Psi(1690,1260)<0$	(CS, CS)	1614 after 1260 cm^{-1}
11	$\Phi(1614,1127)>0$	$\Psi(1690,1127)<0$	(CS, CS)	1614 after 1127 cm^{-1}
12	$\Phi(1614,1050)>0$	$\Psi(1690,1050)<0$	(CS, CS)	1614 after 1050 cm^{-1}
13	$\Phi(1528,1239)<0$	$\Psi(1528,1239)<0$	(COL, CS)	1528 before 1239 cm^{-1}
14	$\Phi(1528,1260)<0$	$\Psi(1528,1260)<0$	(COL, CS)	1528 before 1260 cm^{-1}
15	$\Phi(1528,1127)<0$	$\Psi(1528,1127)<0$	(COL, CS)	1528 before 1127 cm^{-1}
16	$\Phi(1528,1050)<0$	$\Psi(1528,1050)<0$	(COL, CS)	1528 before 1050 cm^{-1}
17	$\Phi(1690,1416)<0$	$\Psi(1690,1416)<0$	(COL, CS)	1690 before 1416 cm^{-1}
18	$\Phi(1690,1377)<0$	$\Psi(1690,1377)<0$	(COL, CS)	1690 before 1377 cm^{-1}
19	$\Phi(1614,1454)<0$	$\Psi(1614,1454)>0$	(CS, COL)	1616 after 1454 cm^{-1}
20	$\Phi(1614,1416)>0$	$\Psi(1614,1416)>0$	(CS, CS)	1616 before 1416 cm^{-1}
21	$\Phi(1614,1377)>0$	$\Psi(1614,1377)>0$	(CS, CS)	1616 before 1377 cm^{-1}
22	$\Phi(1528,1416)<0$	$\Psi(1528,1416)<0$	(COL, CS)	1528 before 1416 cm^{-1}
23	$\Phi(1528,1377)<0$	$\Psi(1528,1377)<0$	(COL, CS)	1528 before 1377 cm^{-1}
24	$\Phi(1454,1260)<0$	$\Psi(1454,1260)<0$	(COL, CS)	1454 before 1260 cm^{-1}
25	$\Phi(1454,1239)<0$	$\Psi(1454,1239)<0$	(COL, CS)	1454 before 1239 cm^{-1}
26	$\Phi(1454,1127)<0$	$\Psi(1454,1127)<0$	(COL, CS)	1454 before1127 cm^{-1}
27	$\Phi(1454,1050)<0$	$\Psi(1454,1050)<0$	(COL, CS)	1454 before1050 cm^{-1}
28	$\Phi(1416,1239)>0$	$\Psi(1416,1239)<0$	(CS, CS)	1416 after 1239 cm^{-1}
29	$\Phi(1416,1127)>0$	$\Psi(1416,1127)<0$	(CS, CS)	1416 after 1127 cm^{-1}
30	$\Phi(1416,1050)>0$	$\Psi(1416,1050)<0$	(CS, CS)	1416 after 1050 cm^{-1}
31	$\Phi(1454,1416)<0$	$\Psi(1454,1416)<0$	(COL,CS)	1454 before1416 cm^{-1}
32	$\Phi(1454,1377)<0$	$\Psi(1454,1377)<0$	(COL, CS)	1454 before1377 cm^{-1}

[a] ν_1 after (before) ν_2 means the intensity change of the band at ν_1 occurs at higher (lower) CS contents than that at ν_2.

the net charge of both collagen and CS is partly screened. Therefore in set A the ionized sulfate group or carboxyl group of CS in a relatively few amount does not interact with collagen through electrostatic bond and only the hydroxyl group of CS form hydrogen bond with C=O group of collagen. However, the net negative charge of CS increases with adding the amount of CS and the electrostatic interaction between sulfate or carboxyl group of CS and cationic residues of collagen appears as a result. It is known that arginine, lysine and histidine have positive charge in neutral medium among all amino acids contained in calf skin collagen. Considering the isoelectric point of arginine, lysine and histidine, then it is supposed that the sulfate or carboxyl group of CS is more likely to interact with ε-amino group of lysine or guanidine group of arginine via electrostatic interaction in the present work.

4. Conclusion

The bands at 1690, 1614, 1528 and 1239 cm^{-1} assigned to collagen and those at 1628, 1416, 1239, 1127 and 1050 cm^{-1} derived from CS are indicative of conformational changes of collagen and molecular interactions between collagen and CS in the Col/CS blends. By virtue of 2D correlation analysis, only hydroxyl group of CS interact with C=O group of collagen through hydrogen bond in set A owing to the charge shielding effect of NaCl. With increasing the amount of CS in set B, electrostatic interactions between collagen and CS appear and the C=O group of CS might form molecular hydrogen bond with amino group of collagen. When adding CS to the collagen solution, C-H bending vibration of collagen varies firstly, then the collagen skeleton, and finally the specific interactions between collagen and CS. In particular the hydrogen bond develops at the lowest content of CS, subsequently ionized sulfate group of CS interacts with ε-amino group of lysine or guanidine group of arginine, and finally the electrostatic interaction between ionized carboxyl group of CS and ε-amino group of lysine or guanidine group of arginine develops. It is considerable that the change of interactions between collagen and CS as a result of various Col/CS ratios could be connected with the physical, chemical or biological properties of the complex. Therefore further study will examine the physicochemical and biological properties of the Col/CS scaffolds produced in a wide range of Col/CS ratio.

Acknowledgement

This research was supported by the National Natural Science Foundation of China (No. 21076129/B060805).

References

Chen, Z. G., Mo, X. M., He, C. L., & Wang, H. S. (2008). Intermolecular interactions in electrospun collagen–chitosan complex nanofibers. *Carbohydrate Polymers*, *72*, 410–418.

Chen, Y. H., Zhang, M., Liu, W. T., & Li, G. Y. (2011). Properties of alkali-solubilized collagen solution crosslinked by N-hydroxysuccinimide activated adipic acid. *Korea-Australia Rheology Journal*, *23*, 41–48.

Cohen, M., Wolfe, R., Mai, T., & Lewis, D. (2003). A randomized, double blind, placebo controlled trial of a topical cream containing glucosamine sulfate, chondroitin sulfate and camphor for osteoarthritis of the knee. *Journal of Rheumatology*, *30*, 523–528.

Denuziere, A., Ferrier, D., & Domard, A. (1996). Chitosan–chondroitin sulfate and chitosan–hyaluronate polyelectrolyte complexes. Physico-chemical aspects. *Carbohydrate Polymers*, *29*, 317–323.

Freyman, T. M., Yannas, I. V., & Gibson, L. J. (2001). Cellular materials as porous scaffolds for tissue engineering. *Progress in Materials Science*, *46*, 273–282.

Garcí a, R., Melad, O., Gómez, C. M., Figueruelo, J. E., & Campos, A. (1999). Viscometric study on the compatibility of polymer–polymer mixtures in solution. *European Polymer Journal*, *35*, 47–55.

Garnjanagoonchorn, W., Wongekalak, L., & Engkagul, A. (2007). Determination of chondroitin sulfate from different sources of cartilage. *Chemical Engineering and Processing*, *46*, 465–471.

Gelman, R. A., & Blackwell, J. (1973). Interaction between collagen and chondroitin-6-sulfate. *Connective Tissue Research*, *2*, 31–35.

Hua, X. H., Li, D., Zhou, F., & Gao, C. Y. (2011). Biological hydrogel synthesized from hyaluronic acid, gelatin and chondroitin sulfate by click chemistry. *Acta Biomaterials*, *7*, 1618–1626.

Huang, H., Malkov, S., Coleman, M., & Painter, P. (2003). Application of two-dimensional correlation infrared spectroscopy to the study of immiscible polymer blends. *Macromolecules*, *36*, 8148–8155.

Jiang, W. H., & Han, S. J. (1998). An improved criterion of polymer–polymer miscibility determined by viscometry. *European Polymer Journal*, *34*, 1579–1584.

Kamata, K., Takahashi, M., Terajima, K., & Nishijima, M. (1995). Spectrophotometric determination of sodium chondroitin sulfate in eye drops after derivatization with 4-amino-3-hydrazino-5-mercapto-1, 2, 4-triazole. *Analyst*, *120*, 2755–2758.

Keskin, D. S., Tezcaner, A., Korkusuz, P., Korkusuz, F., & Hasirci, V. (2005). Collagen-chondroitin sulfate-based PLLA-SAIB-coated rhBMP-2 delivery system for bone repair. *Biomaterials*, *26*, 4023–4034.

Kinneberg, K. R., Nirmalanandhan, V. S., Juncosa-Melvin, N., Powell, H. M., Boyce, S. T., Shearn, J. T., & Butler, D. L. (2010). Chondroitin-6-sulfate incorporation and mechanical stimulation increase MSC-Collagen sponge construct stiffness. *Journal of Orthopaedic Research*, *28*, 1092–1099.

Lamari, F. N., & Karamanos, N. K. (2006). Structure of chondroitin sulfate. *Advances in Pharmacology*, *53*, 33–48.

Lauder, R. M. (2009). Chondroitin sulphate: A complex molecule with potential impacts on a wide range of biological systems. *Complementary Therapies in Medicine*, *17*, 56–62.

Liang, W. H., Kienitz, B. L., Penick, K. J., Welter, J. F., Zawodzinski, T. A., & Baskaran, H. (2010). Concentrated collagen-chondroitin sulfate scaffolds for tissue engineering applications. *Journal of Biomedical Materials Research A*, *94*, 1050–1060.

Maccari, F., Ferrarini, F., & Volpi, N. (2010). Structural characterization of chondroitin sulfate from sturgeon bone. *Carbohydrate Research*, *345*, 1575–1580.

Maruyama, T., Toida, T., Imanari, T., Yu, G. Y., & Linhardt, R. J. (1998). Conformational changes and anticoagulant activity of chondroitin sulfate following its O-sulfonation. *Carbohydrate Research*, *306*, 35–43.

Munakata, H., Takagaki, K., Majima, M., & Endo, M. (1999). Interaction between collagens and glycosaminoglycans investigated using a surface plasmon resonance biosensor. *Glycobiology*, *10*, 1023–1027.

Noda, I. (1989). Two-dimensional infrared-spectroscopy. *Journal of the American Chemical Society*, *111*, 8116–8118.

Noda, I. (1990). 2-Dimensional infrared (2d Ir) spectroscopy-theory and applications. *Applied Spectroscopy*, *44*, 550–561.

Noda, I. (1993). Generalized 2-dimensional correlation method applicable to infrared, Raman and other types of spectroscopy. *Applied Spectroscopy*, *47*, 1329–1336.

Noda, I. (2006). Cyclical asynchronicity in two-dimensional (2D) correlation spectroscopy. *Journal of Molecular Structure*, *799*, 41–47.

Öbrink, B., & Wasteson, Å. (1971). Nature of the interaction of chondroitin-4-sulphate and chondroitin sulphate-proteoglycan with collagen. *Biochemical Journal*, *121*, 227–233.

Öbrink, B. (1973). A study of the interactions between monomeric troprocollagen and glycosaminoglycans. *European Journal of Chemistry*, *33*, 387–400.

Öbrink, B., Laurent, T. C., & Carlsson, B. (1975). The binding of chondroitin sulfate to collagen. *FEBS Letters*, *56*, 166–169.

Pieper, J. S., Oosterhof, A., Dijkstra, P. J., Veerkamp, J. H., & van Kuppevelt, T. H. (1999). Preparation and characterization of porous crosslinked collagenous matrices containing bioavailable chondroitin sulphate. *Biomaterials*, *20*, 847–858.

Ren, Y. Z., Murakami, T., Nishioka, T., Nakashima, K., Noda, I., & Ozaki, Y. (1999). Two-dimensional fourier transform raman correlation spectroscopy studies of polymer blends: Conformational changes and specific interactions in blends of atactic polystyrene and poly (2,6-dimethyl-1,4-phenylene ether). *Macromolecules*, *32*, 6307–6318.

Sakai, S., Otake, E., Toida, T., & Goda, Y. (2007). Identification of the origin of chondroitin sulfate in health foods. *Chemical and Pharmaceutical Bulletin*, *55*, 299–303.

Sionkowska, A., Wisniewski, M., Skopinska, J., Kennedy, C. J., & Wess, T. J. (2004). Molecular interactions in collagen and chitosan blends. *Biomaterials*, *25*, 795–801.

Thomas, V., Dean, D. R., & Jose, M. V. (2007). Nanostructured biocomposite scaffolds based on collagen coelectrospun with nanohydroxyapatite. *Biomacromolecules*, *8*, 631–637.

van Susante, J. L. C., Pieper, J., Buma, P., van Kuppevelt, T. H., van Beuningen, H., van der Kraan, P. M., Veerkamp, J. H., van den Berg, W. B., & Veth, R. P. H. (2001). Linkage of chondroitin-sulfate to type I collagen scaffolds stimulates the bioactivity of seeded chondrocytes in vitro. *Biomaterials*, *22*, 2359–2369.

Wisniewski, M., Sionkowska, A., Kaczmarek, H., Lazare, S., Tokarev, V., & Belin, C. (2007). Spectroscopic study of a KrF excimer laser treated surface of the thin collagen films. *Journal of Photochemistry and Photobiology A: Chemistry*, *188*, 192–199.

Wollenweber, M., Domaschke, H., Hanke, T., Boxberger, S., Schmack, G., Gltesche, K., Scharnweber, D., & Worch, H. (2006). Mimicked bioartificial matrix containing chondroitin sulfate on a textile scaffold of poly (3-hydroxybutyrate) alters the differentiation of adult human mesenchymal stem cells. *Tissue Engineering*, *12*, 345–359.

Yan, M., Li, B., Zhao, X., & Qin, S. (2012). Effect of concentration, pH and ionic strength on the kinetic self-assembly of acid-soluble collagen from walleye pollock (*Theragra chalcogramma*) skin. *Food Hydrocolloids*, doi: 10.1016/j.foodhyd.2012.02.014.

Yannas, I. V., Burke, J. F., Gordon, P. L., Huang, C., & Rubenstein, R. H. (1980). Design of an artificial skin. II. Control of chemical composition. *Journal of Biomedical Materials Research*, *14*, 107–132.

Zhang, M., Wu, K., & Li, G. Y. (2011). Interactions of collagen molecules in the presence of N-hydroxysuccinimide activated adipic acid (NHS-AA) as a crosslinking agent. *International Journal of Biological Macromolecules*, *49*, 847–854.

Zhang, Z. K., Li, G. Y., & Shi, B. (2006). Physicochemical properties of collagen, gelatin and collagen hydrolysate derived from bovine limed split wastes. *Journal of the Society of Leather Technologists and Chemists*, *90*, 23–28.

Zheng, J., Guan, R. Z., & Huang, S. Y. (2008). Comparative studies on the characteristics of the Fourier transform infrared spectra between sturgeon and shark chondroitin sulfates. *Spectroscopy and Spectral Analysis*, *28*, 106–109.

Zhong, S. P., Teo, W. E., Zhu, X., Beuerman, R., Ramakrishna, S., Lin, Y., & Yung, L. (2005). Formation of collagen-glycosaminoglycan blended nanofibrous scaffolds and their biological properties. *Biomacromolecules*, *6*, 2998–3004.